A new approach for the modelling of crystallization processes in impure media using Population Balance Equations (PBE)

François Févotte[*] and Gilles Févotte[**]

** 99, Avenue de Verdun. 92130 Issy les Moulineaux (France)*
*** Ecole des Mines de Saint Etienne, Centre SPIN. 158, Cours Fauriel. 42000 Saint Etienne & Université Lyon 1, 43, Avenue A. Einstein, 69622 Villeurbanne, Cedex (France). fevotte@emse.fr*

Abstract: For obvious industrial and theoretical reasons the problem of accounting for the effect of impurities in the population balance modelling of solution crystallization processes is a very important issue, and yet it has never been reported until today. Meanwhile, several kinetic models are proposed in the literature that relate the effect of impurities on the crystal growth and could be used for PBE modelling. The goal of the present paper is to address this issue and to present a new method, based on characteristics, which is shown to efficiently solve the difficulties raised by the specificity of the mathematical formulation of the Population Balance Equation (PBE) in the presence of impurities. Indeed, as far as hindering effects of the impurities on the crystal growth are concerned, it turns out that the "age" of the particles (i.e. the time they spent in the presence of impurities) might plays a key-role in the overall dynamic crystallization process. Accounting for such a new internal variable required a specific PBE resolution algorithm to be developed and evaluated.

Keywords: Chemical industry, Crystallization, Characteristic curves, Nucleation, Modeling, Population balance equations, Numerical simulation, Batch processes.

1. INTRODUCTION

1.1 Population Balance Equations (PBE) and crystallization

The formalism of Population Balances Equations (PBEs) is a widely used modelling tool in engineering, with applications including crystallization, powder technologies, polymerrization processes, biotechnologies, etc (Ramkrhisna and Mahoney, 2002). PBEs allow describing the time variations of properties of a large number of separate entities, such as particles, bubbles or droplets, interacting with each other and/or with their environment which usually consists of a continuous phase. The dynamics of complex distributed particulate systems is related through the evolution of appropriate distribution functions evolving in a p-dimensional space where p represents the number of internal coordinates required to characterize the particles. Internal coordinates refer to continuous properties of the individual dispersed entities such as size, composition, cristallinity, etc, or to discrete features such as the number of primary crystals in agglomerates or the number of free radicals in a polymerizing particle during emulsion polymerization reactions. In addition to internal coordinates, external coordinates are necessary to describe the physical location of the distributed entities.

As far as dispersed phases are concerned (i.e. separate entities in a continuous fluid phase), the governing equations involve the number density of particles, which is defined as follows:

$$E[n(\boldsymbol{x},\boldsymbol{r},t)] \equiv \psi(\boldsymbol{x},\boldsymbol{r},t), \quad \boldsymbol{x} \in \Omega_x \ , \qquad \boldsymbol{r} \in \Omega_x \tag{1}$$

As already mentioned, external and internal coordinates (i.e. $\boldsymbol{r}$ and $\boldsymbol{x}$, respectively) are necessary to characterize the "location" and the properties of the particles. Equation (1) actually means that the average number of particles in the particle state subspace $dV_x dV_r$ with coordinates $(\boldsymbol{x},\boldsymbol{r})$ is given by $\psi(\boldsymbol{x},\boldsymbol{r},t)\, dV_x dV_r$.

For the sake of simplicity $(\boldsymbol{x},\boldsymbol{r})$ is usually referred to as the particle state and, as outlined by Ramkrishna (2000), it is worth noting that the further definition of PBEs requires the average number density function $\psi(\boldsymbol{x},\boldsymbol{r},t)$to be sufficiently smooth for allowing differentiation with respect to the coordinates and time.

According to the previous definitions, the number $\mathcal{N}$ of particles belonging to a given subset $A_x \subset \Omega_x$ is given by:

$$\mathcal{N}(\boldsymbol{r},t) = \int_{A_x} \psi(\boldsymbol{x},\boldsymbol{r},t) dV_x \tag{2}$$

The previous mathematical formalism will now be applied to the time variations of crystals (i.e. solid particles generated during a crystallization process) characterized by some internal coordinates x. The rate of variation of $\boldsymbol{x}$ is referred to as $\dot{\boldsymbol{X}}$ in the following:

$$\frac{dx}{dt} = \dot{\boldsymbol{X}}(\boldsymbol{x},\boldsymbol{r},\boldsymbol{y},t) \tag{3}$$

where y represents any scalar variables required to quantify the possible interactions (e.g. through heat or mass transfer) between the particles and the continuous phase.

Considering that the following operating conditions are verified:

1. The solution crystallization process takes place in a well mixed batch reactor,

2. new crystals are generated through nucleation phenomena only (i.e. according to the "classical" nucleation theory, the size of new particles appearing in the dispersed phase is the critical size L^* which can be assumed negligible. Agglomeration and breakage of the particles are both neglected),

the population balance equation relating the time variations of the particle state is:

$$\frac{\partial}{\partial t}\psi(\boldsymbol{x},t) + \nabla_x \dot{\mathbf{X}}(\boldsymbol{x},y,t)\,\psi(\boldsymbol{x},t) = h(\boldsymbol{x},y,t) = 0 \qquad (4)$$

with the following boundary conditions:

$$\begin{aligned}\dot{\mathbf{X}}(0,\boldsymbol{x}',y,t)\,\psi(0,\boldsymbol{x}',t) &\cong \dot{\boldsymbol{X}}(L^*,\boldsymbol{x}',y,t)\,\psi(L^*,\boldsymbol{x}',t)\\ &= R_N(y,t)\end{aligned} \qquad (5)$$

where the vector of internal coordinates is decomposed as:

$$\boldsymbol{x} = (L,\boldsymbol{x}')$$

The first assumption above implies that the number density function does not depend on space coordinates while assumption 2 means that, in order to express the source of new particles in the system, one has only to define boundary conditions to account for the expression of the rate(s) of nucleation of crystals (i.e. $h(\boldsymbol{x},y,t)=0$ in (4)).

In the mono-dimensional case where one characteristic size of the particle only is considered (e.g. the diameter L of a fictitious spherical particle exhibiting the same projected area than the crystal under consideration), (4) reduces to the well-known following partial differential equation allowing to compute the time variations of the Crystal Size Distribution (CSD). In the following, y is the supersaturation of the continuous liquid phase σ, defined by (9), which will now be omitted for the sake of simplicity:

$$\begin{cases} \dfrac{\partial\psi(L,t)}{\partial t} + G(t)\dfrac{\partial\psi(L,t)}{\partial L} = 0 & (6)\\ \psi(L,0) = 0 \quad or \quad \psi(L,0) = \psi_{seed} & (7)\\ \psi(0,t) \cong \psi(L^*,t) = \dfrac{R_N(t)}{G(t)} & (8)\end{cases}$$

The initial condition (7) accounts for the possibility of the crystallization to start through primary nucleation (i.e. no solid phase is initially present in the crystallizer) or through seeding. Seeding consists in the introduction of small amount of particles, usually sieved, in the supersaturated solution. The seed particles initiate the crystallization process and are characterized by their size distribution ψ_{seed}.
R_N is the rate of nucleation in #.s^{-1}.m^{-3} and G is the crystal growth rate in m/s.

1.2 Growth rates and impurities

In most published PBE modelling studies —according to McCabe's hypothesis— the growth rate $G(t)$ is assumed not to depend on the particle size but essentially on the driving force of crystallization, the following absolute definition of the supersaturation σ is now defined as:

$$\sigma(t) = C(t) - C^* \qquad (9)$$

where C^* is the equilibrium concentration (i.e. the temperature-dependant solubility of the crystallizing compound) and $C(t)$ is the solute concentration.

Several theoretical or phenomenological expressions can be found in the literature to express the supersaturation-dependency of the growth rate which, more or less, turns out to obey the following kinetic law:

$$G(t) = \frac{dL}{dt} = k_g(C(t) - C^*)^i = k_g\sigma(t)^i \qquad (10)$$

exponent i was shown to depend on the involved growth mechanism(s) which, in particular, depend(s) on the level of supersaturation (Mersmann A, 2002; Mullin J.W., 1993; Chernov, 2004). In practice, consistently with usual theoretical models, most published values of i are given between 1 and 2.

Actually, modeling and control papers published in the field of crystallization engineering deal essentially with pure solute/solvent systems. As far as one considers the context of industrial processes, this is obviously an unrealistic assumption. Indeed, it is worth noting that industrial processes cannot avoid undesirable impurities to be generated during the many chemical reactions preceding the crystallization steps. It is well-known that even minute concentrations of impurities present in the initial solution can affect the crystallization processes (Chernov, 2004; Sangwal, 1996; Wood, 2001) and induce significant reductions of the growth rate (Keshra & Sangwal, 1996; Kubota et al., 2000; Kubota, 2001).

It is also known that impurities can lead to supersaturation thresholds below which the development of crystallization is completely inhibited (see e.g. Sangwal, 2002). To the best of our knowledge, such key-features of "real" industrial crystallization processes (i.e. processes performed in the unavoidable presence of impurities) were investigated through the observation of single crystals, and never described using PBEs. Therefore it remains important to evaluate quantitatively the distribution and the time-variations of the detrimental effects of impurities during crystallization processes.

Now, if one considers the variety of the techniques which were proposed to solve the PBEs in the case of crystallization processes, it appears that few of these methods are based on

the method of characteristics (MOC). It is however known that MOCs avoid numerical diffusion errors and oscillatory solutions caused by the discretization of the involved growth term, especially when steep or discontinuous particulate phenomena take place in suspension (Kumar and Ramkrishna, 1997; Briesen, 2006).

Quamar and Warnecke (2007) have proposed a numerical method for solving PBEs involving nucleation, growth and aggregation processes. The scheme combines a method of characteristics for computing the growth term, with a finite volume technique for calculating aggregation terms. The method is compared to a finite volume scheme through the modelling of "academic" situations for which analytical solutions are available (i.e. combination of crystal growth with aggregation or nucleation). The authors show that the numerical scheme based on MOC is more efficient than pure finite volume schemes, and that it better tracks steep variations of number density functions. This interesting feature of MOC is attributed to the disappearance of the advection term $\partial G\psi/\partial L$ from the main PBE.

Sotowa et al. (2000) compared the numerical resolution of a simple crystallization PBE using a finite difference method and the method of characteristics. The study aimed at evaluating the impact of numerical dispersion on the design of feedback controllers. It was finally concluded that, as far as the simulation of control systems is concerned, the method of characteristics is recommended as a numerical technique for simulating crystallization processes.

More recently, in order to simulate the growth of anisotropic particles, Briesen (2006) proposed a reduced two-dimensionnal PBE model. Here, the MOC approach is used to validate the calculations. The application deals with the crystallization of potassium dihydrogen phosphate which is assumed to exhibit the shape of parallelepipeds terminated by two tetragonal pyramids. However, the simulation assumes initial seeding of the crystallization process only, i.e. no primary or secondary nucleation is taken into account, which is a rather questionable assumption. It should also be noticed that no specific information is reported about the MOC used.

It is the goal of the present paper to address the problem of accounting for the "birthdate" of crystals in the governing crystallization PBE, and to propose a new numerical scheme, based on MOC, for the resolution of the latter PBE. In fact, it is clear that the approach proposed by Kumar and Ramkrishna (1996a,b, 1997) in their series of three papers is much more "advanced" than the approach presented here, in terms of the accuracy of the used size integration technique and with respect to the ability of the method to describe agglomeration and breakage phenomena. Nevertheless, the present algorithm offers another way of considering nucleation phenomena and, through its great simplicity, could be valuable for applications where fast computation is required (i.e. for in-line feedback control applications for example).

2. MODELING THE CRYSTAL GROWTH RATE IN THE PRESENCE OF IMPURITIES.

2.1 The pinning mechanism

With respect to the growth of crystals in pure solvent, the time-averaged advancement velocity of a step in impure media appears to be hindered by the adsorption of impurity species on the growing crystal surface. Indeed, as Fig. 1 schematically shows, during the step advancement, kink sites can be blocked by foreign species that cannot easily be incorporated in the crystal lattice. To allow further crystal growth, the growth-step has to circumvent the pinned impurity, which obviously reduces the overall growth rate. Several models describing such a pinning mechanism were early described in the literature (see e.g. Cabrera & Vermilyea, 1958). Moreover, it is worth noting that many convincing observations of the pinning mechanism were reported, using e.g. advanced imaging techniques such as AFM (Atomic Force Microscopy, see e.g. Land et al., 1999, Thomas et al., 2004).

Kubota-Mullin's model (1995) was proposed to describe the pinning mechanism through Γ, the ratio between the step velocities in pure (u_0) and impure (u) media. Γ is given by the following expression:

$$\Gamma = \frac{u}{u_0} = 1 - \left[\frac{\gamma a}{kT\sigma d}\right]\theta = 1 - \alpha\theta \qquad (11)$$

where γ is the edge free energy, a is the size of the growth unit, T is the absolute temperature, k is the Boltzmann constant and θ is the fraction of coverage of active growing crystal surface by adsorbed impurities, d is the average distance between actives growth sites.

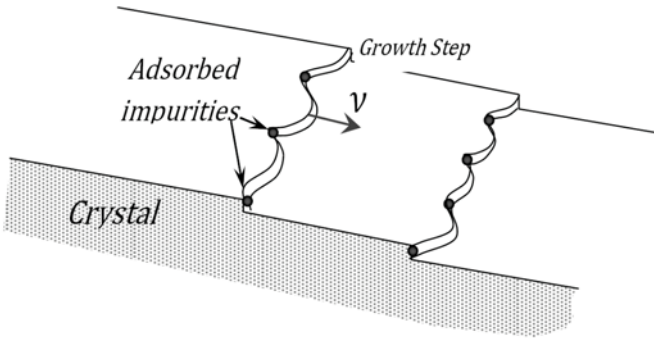

Fig. 1. Adorption of impurities at kink sites on the growing steps after Kubota (2001).

Parameter α is an effectiveness factor which quantifies the efficiency of the impurity specie in hindering the crystal growth. It is very important to notice that α does not only depend on properties of the involved solid, but also on supersaturation.

The coverage of the crystal surface by impurities is itself a stable dynamic process which therefore reaches a steady-state

θ^*. According to the hypotheses set to describe the adsorption process, various theoretical approaches can be used to compute the equilibrium coverage parameter θ^*.

In Kubota-Mullin's Model (Kubota & Mullin, 1995; Kubota et al., 1997), the equilibrium coverage of the growing surface is estimated thanks to Langmuir's adsorption theory:

$$\theta^* = KC_i/(1+KC_i) \tag{12}$$

where K is the Langmuir adsorption constant and C_i is the concentration of impurity.

Even though the adsorption process is often regarded as instantaneous (i.e., the steady-state coverage θ^* is reached instantaneously), it was shown that the dynamics of the adsorption of impurity species on the crystal surface cannot always be neglected. This is the reason why, as a first phenomenological approximation, the transient behavior of the coverage process was proposed by Kubota (2001) to obey a first-order dynamics:

$$\theta = \theta^* (1-\exp(-t/\tau)) \tag{13}$$

where τ is the time constant of the coverage dynamic process.

As the crystal growth rate is usually assumed to be proportional to the step velocity, it finally turns out that G depends on both time and supersaturation while in "usual" crystallization approaches dealing with pure media, G is assumed to depend only on $\sigma(t)$. Combining equations (10) to (13) leads to the following expression where ν is the time at which the crystal surface is set in contact with impure liquid phase (i.e. the time of nucleation):

$$\begin{aligned} G(t) &= k_g \sigma(t)^i \left(1 - \alpha \frac{KC_i}{1+KC_i}\left[1 - \exp\left(-\frac{(t-\nu)}{\tau}\right)\right]\right) \\ &= G_0(t)\left(1 - \alpha \frac{KC_i}{1+KC_i}\left[1 - exp\left(-\frac{(t-\nu)}{\tau}\right)\right]\right) \end{aligned} \tag{14}$$

2.2 Expression of the PBEs accounting for Kubota-Mullin's model of impurities adsorption.

Applying the previous impurity adsorption model (14) is not straightforward as it increases the dimension of the problem: the time $(t-\nu)$ spent by the crystals in contact with impurities should now be accounted for. To this effect, we introduce a population density function ϕ depending on the "classical" variables, L and t, as well as ν:

$$\begin{cases} \dfrac{\partial \phi(L,t,\nu)}{\partial t} + G(t,\nu)\dfrac{\partial \phi(L,t,\nu)}{\partial L} = 0 & (15) \\ \phi(L,0,\nu) = 0 & (16) \\ \phi(0,t,\nu) = \dfrac{R_N(t)}{G(t,\nu)}\delta(t-\nu) & (17) \end{cases}$$

The standard definition of the crystal size distribution can still be retrieved as:

$$\psi(L,t) = \int_0^\infty \phi(L,t,\nu)d\nu = \int_0^t \phi(L,t,\nu)d\nu \tag{18}$$

3. A METHOD OF CHARACTERISTICS FOR SOLVING POPULATION BALANCE EQUATIONS ACCOUNTING FOR IMPURITY EFFECTS.

3.1 A method of characteristics for monodimensional PBEs without impurities.

Actually, the supersaturation $\sigma(t)$ given by Eq. (9), is the driving force of the crystallization process. The decrease of the solute concentration $C(t)$ is caused by the generation of crystals: the molecules of solute initially present in the liquid phase are transferred through crystallization to the dispersed solid phase. The total amount of solid is therefore given by the total volume of solid after integrating the whole CSD:

$$\begin{aligned} C_s(t) &= \rho_s \varphi_p \int_{L^*}^\infty \psi(L,t) L^3 dL \\ &\cong \rho_s \varphi_p \int_0^\infty \psi(L,t) L^3 dL \end{aligned} \tag{19}$$

where ρ_s (kg/m^3) is the density of the solid compound, and φ_p is a volumetric particle shape factor (φ_p is equal to $\pi/6$ if one assumes ideally spherical particles.)

An elementary mass balance of the solute allows computing the evolutions of $C(t)$ and consequently yields $\sigma(t)$ through (9), provided that the solubility curve is known.

Assuming first that the crystallization takes place in pure solvent, the PBE system (6-8) is expressed as follows where the growth rate $G(t)$ is a complex function of physical and kinetic variables depending on $\sigma(t)$ and, through the indirect size-dependency of the solute concentration $C_s(t)$, on the overall current size distribution $\psi(L,t)$:

$$\begin{cases} \dfrac{\partial \psi(L,t)}{\partial t} + G(t)\dfrac{\partial \psi(L,t)}{\partial L} = 0 & (20) \\ \psi(L,0) = 0 & (21) \\ \psi(0,t) = \dfrac{R_N(t)}{G(t)} & (22) \end{cases}$$

In the sequel, it is clear that the process is operated in supersaturated conditions (i.e. $\sigma > 0$), the following condition is therefore always fulfilled:

$$\forall t \in \mathbb{R}^+, \forall \nu \in [0,t\,], \quad G(t) > 0 \tag{23}$$

Now, the following characteristic curves are considered:

$$\forall t \in \mathbb{R}^+, \quad \forall \nu \in [0,t\,] \;, \qquad \tilde{L}_\nu(t) = \int_\nu^t G(t')dt' \tag{24}$$

As represented in Figure 2, the CSD along a given characteristic curve is defined as follows:

$\tilde{\psi}_\nu(t) = \psi\left(\tilde{L}_\nu(t), t\right)$, so that one can write:

$$\frac{d\tilde{\psi}_\nu(t)}{dt} = \frac{\partial\psi\left(\tilde{L}_\nu(t),t\right)}{\partial t} + \frac{d\tilde{L}_\nu(t)}{dt}\ \frac{\partial\psi\left(\tilde{L}_\nu(t),t\right)}{\partial L}$$
$$= \frac{\partial\psi\left(\tilde{L}_\nu(t),t\right)}{\partial t} + G(t)\ \ \frac{\partial\psi\left(\tilde{L}_\nu(t),t\right)}{\partial L}$$
$$\frac{d\tilde{\psi}_\nu(t)}{dt} = 0 \qquad (25)$$

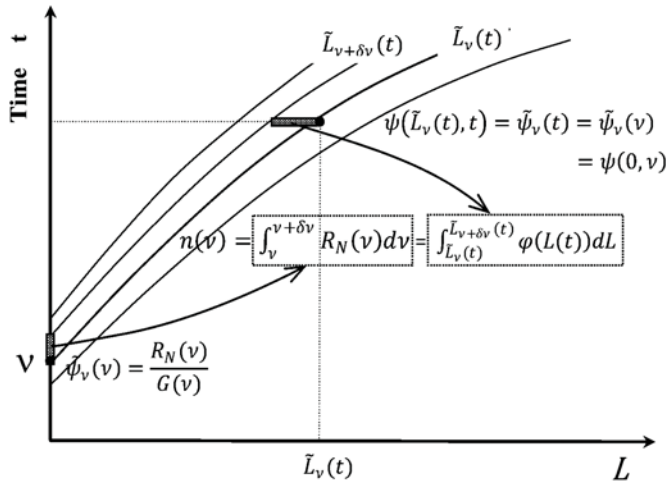

Fig. 2. Schematic representation of the relationship between the number of particles nucleated at time ν and the overall distribution at time t.

It therefore turns out that $\tilde{\psi}_\nu$ does not depend on t, which implies that the solution of (20) is fully determined by the boundary condition (22) and the resolution of (24) describing the time evolutions of the characteristic curves:

$$\forall t \in \mathbb{R}^+,\ \ \forall\, \nu \in [0,t\,]\ \ ,$$
$$\psi\left(\tilde{L}_\nu(t),t\right) = \tilde{\psi}_\nu(\nu) \qquad (26)$$
$$= \tilde{\psi}_\nu(t)$$
$$= \psi(0,\nu)$$
$$\psi\left(\tilde{L}_\nu(t),t\right) = \frac{R_N(\nu)}{G(\nu)} \qquad (27)$$

Now, let us show that equation (27) allows determining the CSD for every size and time, *i.e.* every point (L,t) in the phase space can be represented as $\left(\tilde{L}_\nu(t),t\right)$. To this effect, the following application is considered:

$\lambda_t\colon [0,t\,] \to \mathbb{R}^+, \quad \nu \mapsto \tilde{L}_\nu(t)$

$\forall t \in \mathbb{R}^+$, λ_t is clearly continuous and

$\forall t \in \mathbb{R}^+,\ \forall\, \nu \in [0,t\,]\ ,\ \ \frac{d\lambda_t}{d\nu}(\nu) = -G(\nu)$

which, given (23), shows that λ_τ is strictly decreasing and therefore invertible from $[0,t]$ to $[0,\ \tilde{L}_0(t)]$. It follows that the characteristic curves do not exhibit shock or rarefaction.

A means of computing the distribution density function is therefore given by:

$\forall t \in \mathbb{R}^+, \forall L \in [0,\tilde{L}_0(t)]$,

$$\psi(L,t) = \frac{R_N(\lambda_t^{-1}(L))}{G(\lambda_t^{-1}(L))} \qquad (28)$$

3.2 Semi-discretization of the size population density function.

Considering successive sampling times, the time variable ν is discretized as follows:

$$\forall t \in \mathbb{R}^+, \forall\, \nu \in [0,t\,],\ L_i(t) = \tilde{L}_{\nu_i}(t)$$
$$\Psi_{\mathrm{i}}(\mathrm{t}) = \int_{\mathrm{L_i(t)}}^{\mathrm{L_{i-1}(t)}} \psi(L,t)dL \qquad (29)$$

From (28), and setting the following change of coordinates:

$$\begin{cases} \nu = \lambda_t^{-1}(L) \\ L = \tilde{L}_\nu(t), \qquad \dfrac{dL}{d\nu} = -G(\nu) \end{cases}$$

we get:

$$\Psi_{\mathrm{i}}(\mathrm{t}) = \int_{\mathrm{L_i(t)}}^{\mathrm{L_{i-1}(t)}} \psi(L,t)\ dL$$
$$= \int_{\nu_{\mathrm{i-1}}}^{\nu_{\mathrm{i}}} \psi\left(\tilde{L}_\nu(t),t\right) G(\nu)\ d\nu$$
$$= \int_{\nu_{\mathrm{i-1}}}^{\nu_{\mathrm{i}}} R_N(\nu)\ d\nu \qquad (30)$$

As illustrated by Fig.2, it finally turns out that integrating ψ in size between L_i (t) and L_{i-1} (t), at a given time *t,* amounts to integrating ψ in ν between $\nu_{\mathrm{i-1}}$ and ν_{i} , for a given size, and that the result of this integration does not depend on time t.

Consequently, one simply has now to solve the following two systems which are coupled by the growth rate *G*:

$$\begin{cases} \dfrac{dL_i}{dt}(t) = G(t) \\ L_i(\nu_i) = 0 \end{cases} ; \quad \begin{cases} \dfrac{d\Psi_i}{dt}(t) = 0 \\ \Psi_i(\nu_i) = \int_{\nu_{i-1}}^{\nu_i} R_N(\nu)d\nu \end{cases} \qquad (31)$$

3.3 Time-discretization.

Actually, any time-discretization algorithm can be used to solve jointly the two coupled systems defined by (31). As an example, t can be discretized in the same way as ν, which leads to the very simple numerical scheme displayed below.

Any numerical integration technique can also be used for the computation of the time variations of both L and ψ. The global accuracy of the final numerical solution will mostly be limited by the order of the applied integration scheme.

$k = 0$;
while $t_k < t_{end}$ do

for $i = 1, k-1$ do

$L_i(t_k) = L_i(t_{k-1}) + \int_{t_{k-1}}^{t_k} G(t)\,dt$;

end

$L_k(t_k) = 0$;

$Y_k = \int_{t_{k-1}}^{t_k} R_N(v)\,dv$;

$k = k + 1$;

end

3.4 Method of characteristics for monodimensional PBEs accounting for impurity effects.

Now, in order to account for the distribution of growth rates resulting from the adsorption of impurities, the general system (15-18) is considered. As already explained, the growth rate $G(t)$ is a complex function of physical and kinetic variables depending on time and, through the indirect size-dependency of the solute concentration, on the whole current size distribution:

$$G(t) = f\left(t, v, C^*, C_S \propto \int_0^\infty \phi(L', t, v) L'^3\,(t) dL'\right) \tag{32}$$

where C_S is the overall concentration of crystallized solid given by (19).

The nucleation time of every crystal is introduced in (32) because, as explained in Part 2, the growth rate G now depends on the time spent by the growing crystal surface in the presence of adsorbing impurities.

As in the "classical" case, it is obvious in the following that during the crystallization process the supersaturation remains positive:

$$\forall t \in \mathbb{R}^+, \forall v \in [0, t\,], \quad G(t, v) > 0 \tag{33}$$

Now, let us consider characteristic curves defined as follows:

$$\forall t \in \mathbb{R}^+, \quad \forall (v, \mu) \in [0, t\,]^2,$$
$$\tilde{L}_\mu(t, v) = \int_\mu^t G(t', v) dt' \tag{34}$$

The distribution along a given characteristic curve is noted as follows:

$$\tilde{\phi}_\mu(t, v) = \phi\big(\tilde{L}_\mu(t, v), t, v\big),$$

and one can write:

$$\frac{\partial \tilde{\phi}_\mu(t, v)}{\partial t} = \frac{\partial \phi\big(\tilde{L}_\mu(t, v), t, v\big)}{\partial t} + \frac{\partial \tilde{L}_\mu(t, v)}{\partial t}\,\frac{\partial \phi\big(\tilde{L}_\mu(t, v), t, v\big)}{\partial L}$$
$$= \frac{\partial \phi\big(\tilde{L}_\mu(t, v), t, v\big)}{\partial t} + G(t, v)\,\frac{\partial \phi\big(\tilde{L}_\mu(t, v), t, v\big)}{\partial L} \tag{35}$$

$$\frac{\partial \tilde{\phi}_\mu(t, v)}{\partial t} = 0 \tag{36}$$

As before, it therefore turns out that $\tilde{\phi}_\mu(t, v)$ does not depend on t. It can also be concluded that:

$$\forall t \in \mathbb{R}^+, \quad \forall (v, \mu) \in [0, t\,]^2,$$

$$\phi\big(\tilde{L}_\mu(t, v), t, v\big) = \tilde{\phi}_\mu(t, v) \tag{37}$$
$$= \tilde{\phi}_\mu(\mu, v)$$
$$= \phi(0, \mu, v) \tag{38}$$
$$\phi\big(\tilde{L}_\mu(t, v), t, v\big) = \delta(\mu - v)\frac{R_N(\mu)}{G(\mu, v)} \tag{39}$$

3.5 Semi-discretization of the size population density function taking the nucleation time into account.

The time variable μ is discretized considering successive sampling times: $\mu \in \{\mu_i, i \in \mathbb{N}\}$, and one can define the following distribution function:

$$\forall t \in \mathbb{R}^+, \forall v \in [0, t\,]$$
$$L_i(t) = \tilde{L}_{\mu_i}(t, v) \tag{40}$$
$$\Phi_i(t, v) = \int_{L_i(t,v)}^{L_{i-1}(t,v)} \phi(L, t, v) dL$$
$$\Psi_i(t) = \int_0^t \Phi_i(t, v) dv \tag{41}$$

Using (40) and setting:
$$\begin{cases} \mu = \lambda_{t,v}^{-1}(L) \\ L = \tilde{L}_\mu(t, v), \end{cases}$$

$$L = \tilde{L}_\mu(t, v), \ \frac{dL}{d\mu}(\mu) = -G(\mu, v) \tag{42}$$

yields:

$$\Phi_i(t, v) = \int_{L_i(t,v)}^{L_{i-1}(t,v)} \phi(L, t, v) dL \tag{43}$$
$$= \int_{\mu_{i-1}}^{\mu_i} \phi\big(\tilde{L}_\mu(t, v), t, v\big) G(\mu, v) d\mu \tag{44}$$

$$\Phi_i(t,\nu) = \int_{\mu_{i-1}}^{\mu_i} \delta(\mu-\nu)\, R_N(\mu)\, d\mu \quad (45)$$

$$= \begin{cases} R_N(\nu) & if\ \nu \in [\mu_{i-1}\,;\mu_i] \quad (46) \\ 0 & otherwise \quad (47) \end{cases}$$

It follows that:

$$\Psi_i(t) = \int_0^t \Phi_i(t,\nu)d\nu = \int_{\mu_{i-1}}^{\mu_i} R_N(\nu)d\nu \quad (48)$$

The following two systems are thus obtained which are coupled by the growth rate G:

$$G(t) = f\left(t, \mu_i, C^*, C_s \propto \sum_i \Psi_i(\mu_i)\, L_i^3(t)\right) \quad (49)$$

$$\begin{cases} \frac{dL_i}{dt}(t) = G(t) \\ L_i(\mu_i) = 0 \end{cases} \quad \begin{cases} \frac{d\Psi_i}{dt}(t) = 0 \quad (50) \\ \Psi_i(\mu_i) = \int_{\mu_{i-1}}^{\mu_i} R_N(\mu)\, d\mu \quad (51) \end{cases}$$

The principle of the resolution numerical method is the same as previously (see Fig. 2 and Part 3.3).

4. APPLICATION: SIMULATION OF THE CRYSTALLIZATION OF CITRIC ACID MONOHYDRATE IN THE PRESENCE OF IMPURITIES.

In order to illustrate the resolution method, the crystallization of citric acid monohydrate is simulated using kinetic data previously published by Févotte *et al*. (2007). In the absence of reported experimental results in impure media, the parameters of the Kubota-Mullin model were set arbitrarily in order to compare the features of crystallization operations performed with and without impurities. The corresponding parameters are summarized in Table (1).

In the following, no effect of the impurities on the nucleation kinetics is simulated, which is probably a very rough assumption. Actually published data about nucleation in the presence of impurities are really lacking and the goal here is rather to show the usefulness of the resolution method than to investigate real solute/solvent/impurity systems.

Isothermal desupersaturation crystallization operations were simulated at 15°C. In order to initiate the crystallization in the supersaturated zone (i.e. $C_{init.}$ >C* at 15°C)), a seed mass of 10 kg (2% of the expected final mass of solid) is supposed to be introduced in a 1 m^3 pilot-scale well-mixed crystallizer initially feed with a supersaturated citric acid solution. The intial solute concentration is: C_{init} = 1.825 kg/kg water. After seeding, the number of particles increases, due to secondary nucleation, and the initial supersaturation is consumed through the growth of crystals. Despite the adsorption of impurity species at the crystal surfaces, the overall concentration C_i is assumed to remain constant during the crystallization (i.e. the amount of adsorbed molecules is clearly negligible with respect to the dissolved impurities.

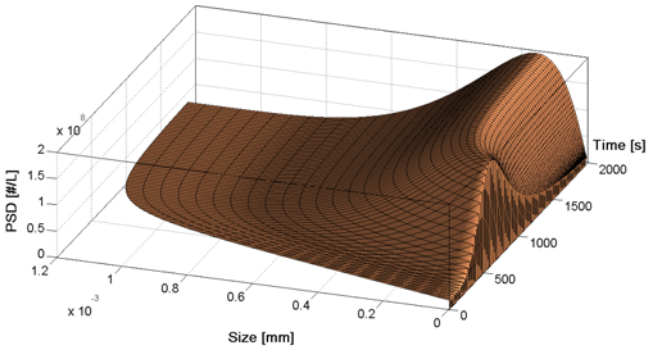

Fig. 3. Simulation of seeded isothermal crystallization of citric acid monohydrate in pure water at 15°C.

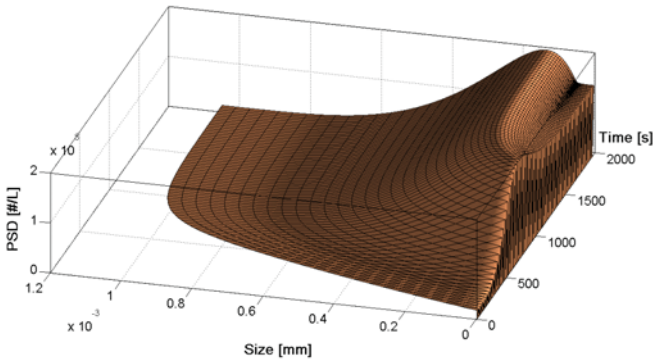

Fig. 4. Simulation of seeded isothermal crystallization of citric acid monohydrate in water and in the presence of impurity at 15°C. The parameters of Kubota-Mullin's are given in Table 1.

As one can see in Figs. 3 and 4, the computed CSD is smooth and does not exhibit oscillatory behaviour, even when coarse time intervals are used for the numerical simulation. As expected, the presence of impurities has a clear effect on the development of the CSD. Fig. 3 shows that the size of the biggest particles obtained in pure water is about 1.2 mm while it is only 1 mm in the presence of impurities (Fig.4). However, Fig.5c shows that the main difference between the two final CSDs can be observed in a rather significant increase in the number of fines which is expected to have a very detrimental effect on the the downstream operation such as filtration.

It turns out that the most significant effects of the impurities on the development of the batch process arise from the reduction of the supersaturation decrease, as displayed in Fig.5a.

Indeed, as outlined in Part 1.2, due to the pinning mechanism, the level of supersaturation remains higher when impurities are present in the crystallizing solution. As during the present simulation no impurity effect is assumed to affect the secondary nucleation of new citric acid particles, higher levels of supersaturation lead to a much higher overall

number of particles (Fig.5d) while, due to growth rate reductions and to the final supersaturation threshold outlined previously, the overall production of solid is clearly reduced. Figure 5b shows that only 70% of the expected solid is obtained at the end of the batch process performed in the presence of impurities (0.5 kg/L of crystals was expected from the selected values of C_{init} and C*).

Table 1. Kinetic equations and parameters used for the simulation of the crystallization of Citric Acid monohydrate.

$$\frac{dL}{dt} = G(t) = k_g(C(t) - C_m^*)^i$$
$$= 7.18\ 10^{-6}(C(t) - C_m^*)^{1.58} \quad (52)$$
$$R_N(t) = K_2\ C_S(t)^{i_m}(C(t) - C_m^*)^{j_m}$$
$$= 1.72\ 10^8\ C_S(t)^{0.47}(C(t) - C_m^*)^{1.14} \quad (53)$$

where $R_N(t)$ is the rate of secondary nucleation of monohydrate citric acid,

K_2 is a "lumped" kinetic constant for secondary nucleation,

C_m^* is the solubility of monohydrate citric acid at 15°C (1.35 kg/kg of water),

i & j_m are exponents expressing the supersaturation dependency of the growth rate and nucleation rate,

i_m is the exponent accounting for the impact of solid already present in suspension on the secondary nucleation rate.

$$C_s(t) = \rho_s \varphi_p \int_{L^*}^{\infty} \psi(L,t) L^3 dL$$

where ρ_s= 1545 kg/m^3

φ_p= π/6 (spherical particles)

Parameters of Kubota-Mullin's Model:

K = 1 m^3/kg
C_i = 0.01 kg/m^3
τ = 500 s
α = 10/σ

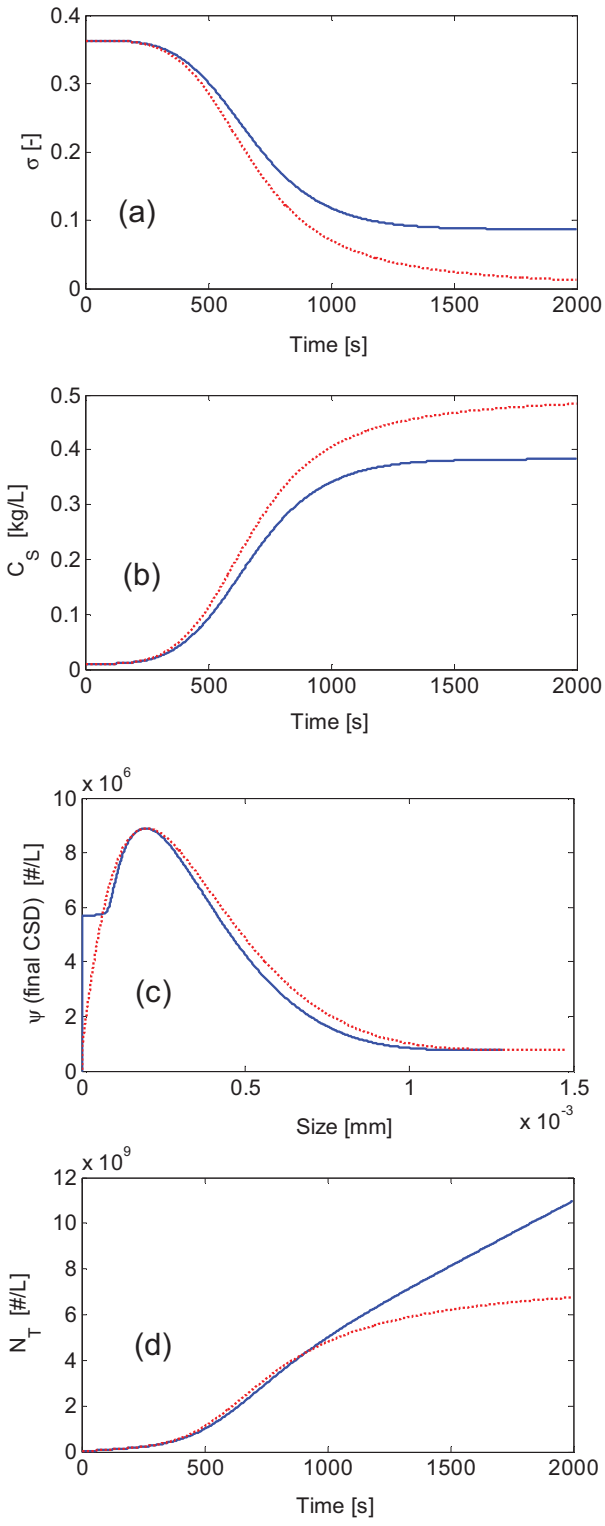

Fig. 5 . Simulation of seeded isothermal crystallization of citric acid monohydrate in water with (dotted line) and without (continuous line) the presence of impurities, at 15°C.

(a) Desupersaturation profile. (b) Generation of total crystallized solid during time. (c) Nucleation rate assuming negligible effect of the impurity species on the generation of particles. (d) Overall number of crystals.

5. CONCLUSIONS

A method of characteristics for the resolution of population balance equations was developed and evaluated using published kinetic data on the crystallization of citric acid in water. The method can be applied to crystallization processes without agglomeration and breakage, and it is intended to allow the simulation of growth rate reductions observed during solution crystallizations performed in the presence of industrial impurities.

Indeed, the effect of impurities was shown by Kubota and Mullin (1995) to depend on the time spent by every crystal in the impure liquid medium and, consequently, to depend on the "age" of the crystals. Such a particular problem requires accounting for an additional time variable in the expression of the PBEs and finding a way of solving the resulting PBE system.

From a physical viewpoint, the simulation results are shown to be consistent and demonstrate the ability of the model to simulate the development industrial crystallization processes in the presence of impurities. Such simulation could be applied, for example, to the design of optimal temperature trajectories aimed at minimizing the detrimental effect of the concentration of impurities on the yield of industrial crystallization operations.

As outlined by several authors (Kumar and Ramkrishna, 1997; Briesen, 2006), despite the apparent simplicity of these two processes, the discretization of crystal nucleation and growth raises numerical diffusion and stability issues which arise from the hyperbolic features of the governing equations (6) to (8). From this latter viewpoint it is clear that the proposed resolution method allows one to account for nucleation and growth rates in a very straightforward way.

NOMENCLATURE

C	Solute concentration	kg solute/kg solvent
C^*	Solubility concentration	kg solute/kg solvent
C_i	Impurity concentration	kg.m^{-3}
C_S	Solid concentration	kg.m^{-3}
G	Growth rate	m. s^{-1}
i	Exponent of the supersaturation dependency of the crystal growth rate	[-]
i_m	Exponent of the dependency of the nucleation rate on the concentration of solid in suspension	[-]
j_m	Exponent of the supersaturation dependency of the nucleation rate	[-]
K	Langmuir's constant	m^3. kg^{-1}
k_g	Growth rate constant	[-]
K_2	Kinetic nucleation parameter	
L	Particle size	m
$\mathcal{N}(\boldsymbol{r},t)$	Number of particles at time t in a given subset	#.m^{-3}
R_N	Nucleation rate	#.s^{-1}.m^{-3}
t	Time	s
u	Step velocity	m. s^{-1}
	Greek letters	
α	Impurity effectiveness factor	[-]
θ	Fraction of coverage of growing crystal surface by adsorbed impurity	[-]
θ^*	Fraction of coverage of growing crystal surface by adsorbed impurity at the equilibrium	[-]
ν	Nucleation time	s
σ	Supersaturation	[-]
τ	Adsorption time constant	s
$\psi(L,t)$	Population density function	#.m^{-1}.m^{-3}

REFERENCES

Briesen, H. (2006) Simulation of crystal size and shape by means of a reduced two-dimensional population balance model. *Chem. Engng. Sci.,*61, 104-112.

Cabrera, N. and Vermilyea, D.A. (1958). in *Growth and Perfection of Crystals*, New York, 393 p.

Chernov, A.A. (2004). Notes on interface growth kinetics 50 years after Burton, Cabrera and Frank. *J. of Crystal Growth,* 264(4), 499-518.

Févotte, G., Caillet, A. and Sheibat-Othman, N. (2007). A population balance model of the solution-mediated phase transition of citric acid. *AIChE Journal*, 53(10), 2578-2589.

Kubota, N. (2001). Effect of Impurities on the Growth Kinetics of Crystals. *Cryst. Res. Technol*., 36(8-10), 749–769.

Kubota, N. (2001). Effect of Impurities on the Growth Kinetics of Crystals. *Cryst. Res. Technol*., 36, 749–769.

Kubota, N., Yokota, M. and Mullin, J.W. (2000). The combined influence of supersaturation and impurity concentration on crystal growth. *J. Crystal Growth*, 212(3-4), 480-488.

Kubota, N. and Mullin, J.W. (1995). A kinetic model for crystal growth from aqueous solution in the presence of impurity. *J. Crystal Growth,* 152(3), 203-208.

Kubota, N., Yokota, M. and Mullin, J.W. (1997). Supersaturation dependence of crystal growth in solutions in the presence of impurity. *J. Crystal Growth*, 182(1-2), 86-94.

Kumar, S. and Ramkrishna, D. (1996). On the solution of population balance equations by discretization--I. A fixed pivot technique, *Chem. Engng. Sci.,* 51, 8, 1311-1332.

Kumar,S., and Ramkrishna, D. (1996). On the solution of population balance equations by discretization--II. A

moving pivot technique, *Chem. Engng. Sci.,* 51, 8, 1333-1342.

Kumar, S. and Ramkrishna, D. (1997). On the solution of population balance equations by discretization- III. Nucleation, growth and aggregation of particles, *Chem. Engng. Sci*. 52, 24, 4659-4679.

Land, T.A., Martin, T.L., Potapenko, S., Palmore, G.T., De Yoreo, J.J. (1999). Recovery of surfaces from impurity poisoning during crystal growth. *Nature*, 399, 442-445.

Mersmann, A. (2002). Fundamentals of crystallization. *Crystallization Technology Handbook,* 2nd Ed., New York: Marcel Dekker.

Qamar,S.; Warnecke,G. (2007). Numerical solution of population balance equations for nucleation, growth and aggregation processes, *Comp. & Chem. Engng*. 31, 1576-1589.

Mullin, J.W. (1993). *Crystallization,* 3rd Ed., London (UK): Butterworth-Heinemann,

Ramkrishna, D. (2000). Population Balances: *Theory and Applications to Particulate Systems Engineering,* Academic Press.

Ramkrishna, D.; Mahoney, A.W. (2002). Population balance modelling. Promise for the future. *Chem. Engng. Sci*., 57, 595-606.

Sangwal, K. (1996). Effects of impurities on crystal growth processes. *Progress in Crystal Growth and Characterization of Materials*, 32(1-3), 3-43.

Sotowa, K.I., Naito, K., Kano, M., Hasebe, S., Hashimoto, I. (2000). Application of the method of characteristics to crystallizer simulation and comparison with finite difference for controller performance evaluation. *J. of Process Control*, 10, 203-208.

Thomas, T.N., Land, T.A., Martin, T., Casey, W.H., DeYoreo, J.J. (2004). AFM investigation of step kinetics and hillock morphology of the {1 0 0} face of KDP. *J. Crystal Growth,* 260(3-4), 566-579.

Wood, W.M.L. (2001). A bad (crystal) habit--and how it was overcome. *Powder Technology*, 121(1), 53-59.

ACKNOWLEDGEMENTS

We greatly acknowledge the French research agency ANR for the support granted to the project “IPAPI” (Improving the Properties of Active Pharmaceutical Ingredients), ref. 07-BLAN-0183